ELSEVIER

Materials Science and Engineering A 438–440 (2006) 427–430

MATERIALS SCIENCE & ENGINEERING A

www.elsevier.com/locate/msea

Mechanically induced phase combination in shape memory alloys by Chebyshev collocation methods

L.X. Wang [a,*], Roderick V.N. Melnik [b]

[a] *MCI, Faculty of Science and Engineering, University of Southern Denmark, Sonderborg DK-6400, Denmark*

[b] *Center for Coupled Dynamics and Complex Systems, Wilfrid Laurier University, 75 University Avenue West, Waterloo, Ont., Canada N2L 3C5*

Received 22 April 2005; received in revised form 31 October 2005; accepted 28 February 2006

Abstract

A mathematical model is constructed to simulate the martensitic phase combinations in shape memory alloy samples. Governing equations are obtained on the basis of the momentum balance law and a modified Landau–Ginzburg free energy functional. The Chebyshev collocation method is applied for the numerically analysis of the constructed model. Computational experiments with given mechanical loadings and boundary conditions demonstrate that the phase combinations between martensite variants in the 2D shape memory alloy samples can be successfully simulated with the developed methodology.

Keywords: Rectangular martensite variants; Phase combinations; Ginzburg–Landau theory; Chebyshev collocation method

1. Introduction

It is known that a phase combination in the shape memory alloys (SMAs) is the major cause of the dramatic change of their physical properties under appropriate thermo-mechanical loadings. Many instructive investigations have been carried out towards a better understanding of the microstructure and phase combinations in ferroelastic materials ([1–4] and references therein). These investigations have been carried out within the same mathematical framework, in which the microstructure in the material is associated with an energy minimizer of a variational problem. Hence, one of the most popular approaches to the problem of computing the microstructure is based on the direct energy minimization, along which a free energy functional is constructed to characterize the martensite and austenite states by its local minima at different temperatures. In such cases, it is expected that the global minimum of the bulk energy gives the microstructure and several laminated structures were successfully simulated using these ideas ([1–3] and references therein). Another approach to the problem is to apply the time-dependent Ginzburg–Landau theory. The essential element of this approach is to characterize the martensite and austenite by a modified Ginzburg–Landau free energy functional, by taking into account the dissipation while ignoring the kinetic terms. In the end, this approach gives the stable microstructure in the material, while the transient processes give the evolution of the microstructure ([5–8] and references therein). Both approaches mentioned above are essentially mesoscale approaches. The task of extending these approaches to the modelling of microstructure-dependent multiscale phase combinations is far from trivial, due to difficulties of enforcing non-periodic boundary conditions and other factors resulting from a multiscale nature of the problem.

In this paper, we propose an approach to model phase combinations in SMA samples focusing at the macroscale. In the proposed model, the modified Ginzburg–Landau free energy functional is adapted, in way similar to the approach mentioned above, to characterize the martensite and austenite by its local minima. However, instead of applying the time-dependent Ginzburg–Landau theory for the dynamic simulation, or directly minimizing the bulk energy in the SMA sample to get the global energy minimizer, we employ the nonlinear elastic theory to obtain the governing equations for displacement distributions. In this model, the constitutive relationships are derived from the free energy functional using the thermodynamic equilibrium conditions. By applying the proposed technique, the problem can be reduced to an usual elastic problem on a macroscale. The developed model is strongly nonlinear. It allows a robust implementation of all typical boundary conditions.

* Corresponding author. Tel.: +45 6550 1686; fax: +45 6550 1660.
E-mail address: wanglinxiang@mci.sdu.dk (L.X. Wang).

0921-5093/$ – see front matter © 2006 Elsevier B.V. All rights reserved.
doi:10.1016/j.msea.2006.02.156

2. Mathematical model of phase combinations

To model phase combinations in SMA samples at the macroscale, we start from the conservation laws for mass and momentum of the elasticity theory. In its general form, stationary distributions of strains can be described by the static Navier equations as follows:

$$\frac{\partial\sigma_{11}}{\partial x}+\frac{\partial\sigma_{21}}{\partial y}+f_x=0, \qquad \frac{\partial\sigma_{12}}{\partial x}+\frac{\partial\sigma_{22}}{\partial y}+f_y=0, \tag{1}$$

where $\sigma=\{\sigma_{ij}\}$ is the stress tensor, and $f=(f_x, f_y)^{\mathrm{T}}$ are mechanical loadings in the x and y directions, respectively.

One of the key tasks in constructing the model for phase combinations is to obtain constitutive relationships that are able to characterize both the martensite variants at low temperature as well as the austenite phase at high temperature. In what follows, we exemplify our discussion with the model that describes phase combinations of rectangular martensitic variants, which could be induced by the square-to-rectangular transformation. This transformation could be regarded as a 2D analog of the cubic-to-tetragonal and tetragonal-to-orthorhombic transformations observed in general 3D cases (in the alloys like in Nb_3Sn, InTl, FePd as well as in some copper-based SMAs, see [5–8] and references therein). In the context of SMAs, researchers have successfully constructed several constitutive laws for SMA dynamic simulations, specifically for the case of square-rectangular transformations [5,9,10].

For the current simulation of 2D phase combinations with a given temperature distribution, the free energy functional can be chosen based on the modified Ginzburg–Landau theory in a way similar to those discussed in [5–9] (see also references therein):

$$\Psi(\Delta\theta,\varepsilon)=\frac{a_1}{2}e_1^2+\frac{a_3}{2}e_3^2+F_{\mathrm{l}}+F_{\mathrm{g}},$$

$$F_{\mathrm{l}}=\frac{a_2}{2}\Delta\theta e_2^2-\frac{a_4}{4}e_2^4+\frac{a_6}{6}e_2^6,\quad F_{\mathrm{g}}=\frac{d_2}{4}\left[\left(\frac{\partial e_2}{\partial x}\right)^2+\left(\frac{\partial e_2}{\partial y}\right)^2\right], \tag{2}$$

where a_i, $i=1,\ldots,6$, and d_2 are the material-specific coefficients and $\Delta\theta=\theta-\theta_0$ is the temperature difference between the material temperature and the reference temperature θ_0. Variables e_1, e_2, and e_3 are dilatational, deviatoric, and shear components of the strains, respectively, defined as follows:

$$e_1=\frac{\eta_{11}+\eta_{22}}{\sqrt{2}}, \qquad e_2=\frac{\eta_{11}-\eta_{22}}{\sqrt{2}}, \qquad e_3=\frac{\eta_{12}+\eta_{21}}{2}, \tag{3}$$

where the Cauchy–Lagrangian strain tensor η is given by its components as follows (with the repeated-index convention used):

$$\eta_{ij}(x,t)=\frac{\partial u_i(x,t)/\partial x_j+\partial u_j(x,t)/\partial x_i}{2}, \tag{4}$$

where u_i is the displacement in the ith direction in the coordinate system and x is the coordinates of a material point in the domain of interest. In the presented formulation, the deviatoric strain e_2 is chosen as the order parameter.

Having the free energy functional, it is easy to get the constitutive relationships using the thermodynamical equilibrium conditions:

$$\sigma=\frac{\delta\Psi(\Delta\theta,\varepsilon)}{\delta\eta}. \tag{5}$$

To close the mathematical model, problem-specific boundary conditions should be applied. Such conditions are discussed in Section 4. Here, we note only that since the governing equations are now formulated in terms of the displacements, the implementation of the mechanical boundary conditions is straightforward.

3. Numerical methodology

Prior to the numerical solution of the model given by Eqs. (1) and (5), it is convenient to recast it as follows:

$$\frac{\partial\sigma_{11}}{\partial x}+\frac{\partial\sigma_{12}}{\partial y}+f_x=0, \qquad \frac{\partial\sigma_{12}}{\partial x}+\frac{\partial\sigma_{22}}{\partial y}+f_y=0,$$

$$\sigma_{11}=\frac{\sqrt{2}}{2}\left(a_1e_1+a_2\Delta\theta e_2-a_4e_2^3+a_6e_2^5-\frac{d_2}{2}\nabla^2e_2\right),$$

$$\sigma_{12}=\sigma_{21}=\frac{1}{2}\left(a_3e_3\right),$$

$$\sigma_{22}=\frac{\sqrt{2}}{2}\left(a_1e_1-a_2\Delta\theta e_2+a_4e_2^3-a_6e_2^5+\frac{d_2}{2}\nabla^2e_2\right), \tag{6}$$

where the constitutive relations are considered as independent equations in this system while the stress components are considered here as independent variables to be solved for.

For the spatial discretization, the Chebyshev pseudospectral approximation (e.g. [12]) is employed here on a set of Chebyshev points (x_i, y_j) distributed within the 2D sample with size $[-1,1]\times[-1,1]$:

$$x_i=\cos\left(\frac{\pi i}{N}\right), \qquad y_j=\cos\left(\frac{\pi j}{N}\right), \quad i,j=0,1,\ldots,N, \tag{7}$$

where $N+1$ is the number of nodes. Using the discretization, the stress and velocity distributions in the sample can be approximated by the following linear combination:

$$f(x,y)=\sum_{i=0}^{N}\sum_{j=0}^{N}f_{i,j}\phi_i(x)\phi_j(y), \tag{8}$$

where $f(x, y)$ could be either stresses or displacements, $f_{i,j}$ the function value at (x_i, y_j), $\phi_i(x)$ and $\phi_j(y)$ are the ith and jth Lagrange interpolating polynomials along x and y directions, respectively.

Using the above function approximation, the derivatives of the function with respect to x and y can be written in the following matrix form as in [11]:

$$\left.\frac{\partial f(x,y)}{\partial x}\right|_{x_i,y_j}=\mathbf{D}_x\mathbf{F}, \qquad \left.\frac{\partial f(x,y)}{\partial y}\right|_{x_i,y_j}=\mathbf{D}_y\mathbf{F}. \tag{9}$$

By approximating all the differential operators in the governing Eq. (6), the system can be discretized and converted into a set of nonlinear algebraic equations, which can be solved by the bi-conjugate gradient iteration method.

4. Numerical results

To demonstrate the capability of the constructed model, the martensite combination under various mechanical loadings have been simulated. In what follows, we report a representative numerical experiment. The simulation has been carried out for a $Au_{23}Cu_{30}Zn_{47}$ sample with size 2 cm × 2 cm. For this specific material, physical parameters are taken the same as in [10] (given there for the 1D case). For the 2D model (6), there are no 2D experimental values for the physical parameters. Here, we take the values $a_1 = 2a_2$, $a_3 = a_2$, as suggested in [6,9]. We choose the coefficient for the Ginzburg term as $d_2 = a_2 \times 10^{-6}$, and the sample temperature is assumed to be $\theta = 210\,^\circ$.

Boundary conditions for the current numerical experiment are as follows:

$$\frac{\partial u_1}{\partial y} = 0, \quad u_2 = 0, \text{ at } y = \pm 1, \qquad \frac{\partial u_2}{\partial x} = 0,$$
$$u_1 = 0, \text{ at } x = \pm 1, \tag{10}$$

and distributed mechanical loadings are given by:

$$f_x = 2000 \times \text{sign}(x)\ (\text{g}/(\text{ms}^3\ \text{cm})),$$
$$f_y = 2000 \times \text{sign}(y)\ (\text{g}/(\text{ms}^3\ \text{cm})),$$

where $\text{sign}(t) = 1$ if $t > 0$ and $\text{sign}(t) = -1$ if $t < 0$ (with t being either x or y).

Starting from the initial guess (all zero), the final distribution of u_1 and u_2 is plotted when the difference between two subsequent iterations is smaller than 10^{-6}. We have used 18 nodes in each direction.

It is known that there are two rectangular martensitic variants characterized by the free energy functional F_1. The results of simulation are presented for the order parameter e_2 calculated from u_1 and u_2 (see Fig. 1). The combination of martensite variants under the given mechanical loading can be seen clearly at the mesh plot of e_2 on the Chebyshev collocation points (Fig. 1(a)). The entire sample is symmetrically occupied by four subdomains, two of them with e_2 around 0.11 and another two around −0.11 (Fig. 1(b)). These two values correspond to the two minima of the free Landau energy functional F_1, which could be calculated by

$$\frac{\partial F_1}{\partial e_2} = 0, \quad e_2 = \pm\sqrt{\frac{a_4 + \sqrt{a_4^2 - 4a_2a_6\Delta\theta}}{2a_6}} \tag{11}$$

with the given temperature difference $\Delta\theta = 2\,^\circ$. One can easily obtain that the local minimum of the Landau free energy func-

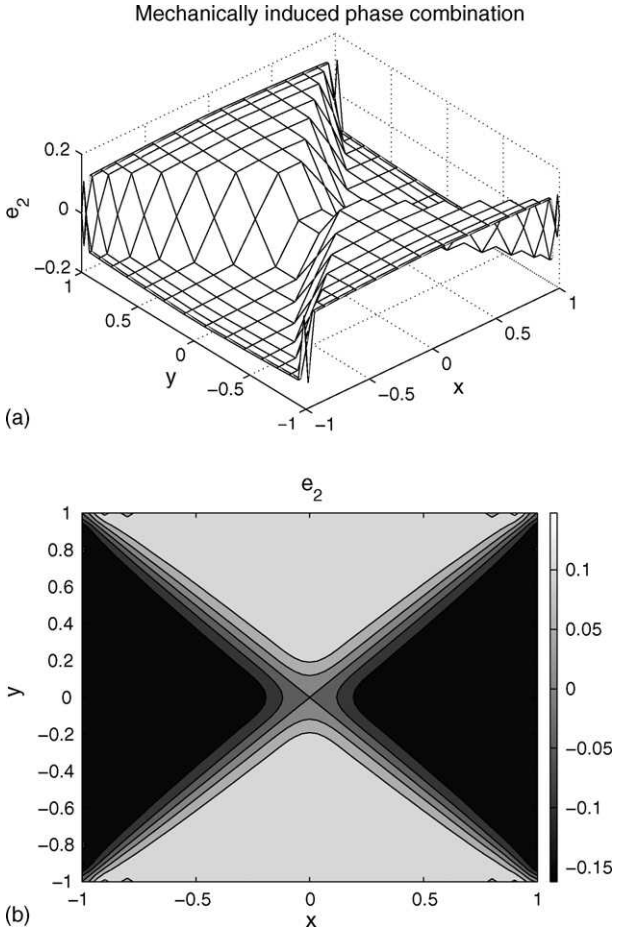

Fig. 1. Simulation results of the phase combination in a SMA patch. (a) Mesh plot of e_2 and (b) contour plot of interpolated e_2.

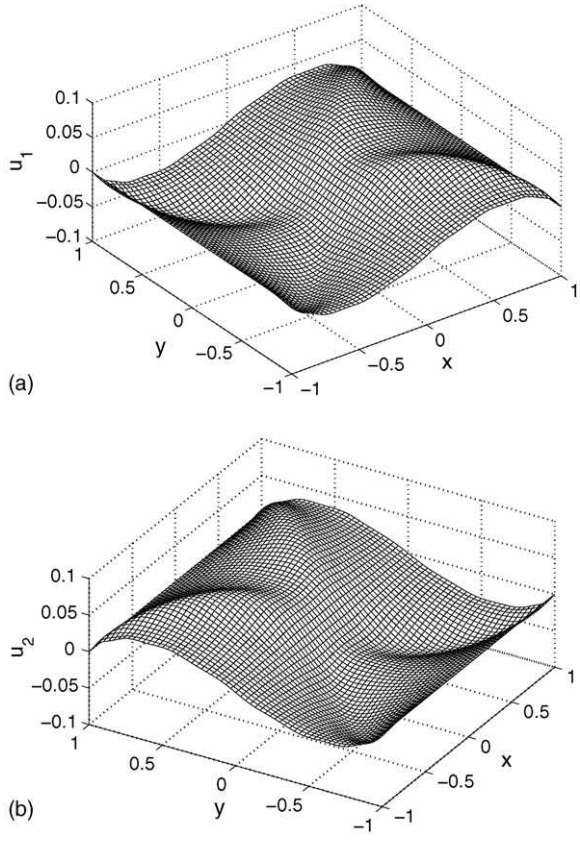

Fig. 2. Simulation results of phase combination in a SMA patch. (a) Displacement u_1 and (b) displacement u_2.

tional is at $e_2 = \pm 0.1148$. This shows that the phase combination obtained here by the nonlinear elasticity approach coincides with those obtained with the energy minimization approach. The difference is that we are able to incorporate here the mechanical boundary conditions in a straightforward manner.

Next, in order to present displacements, they are interpolated on the Chebyshev collocation points, and then mapped onto a more dense grid (60 nodes along each direction). The values of e_2 are re-calculated on the dense grid using the second order finite difference method. The contour plot of this interpolated e_2 shows also the interfaces between martensite variants. The two interpolated displacement components are also presented in Fig. 2. The symmetry patterns in u_1 and u_2 is clearly observed on both plots. Note also that if u_1 is rotated 45° counterclockwise, it will coincide with u_2. This agrees well with the physics of the problem discussed in [5,6].

These computational experiments demonstrate that the constructed model is capable to simulate successfully phase combinations in SMA samples with square-to-rectangular phase transformations.

References

[1] J.L. Ericksen, J. Solids Struct. 22 (1986) 951–964.
[2] R. Ball, M. James, Arch. Ration. Mech. Anal. 100 (1988) 13–52.
[3] M. Luskin, Acta Numer. 5 (1996) 191–256.
[4] S. Muller, Lect. Notes Math. 1713 (1999) 85–210.
[5] T. Lookman, S. Shenoy, D. Rasmussen, A. Saxena, A. Bishop, Phys. Rev. B 67 (2003) 024114.
[6] A. Jacobs, Phys. Rev. B 61 (10) (2000) 6587–6595.
[7] T. Ichitsubo, K. Tanaka, M. Koiva, Y. Yamazaki, Phys. Rev. B 62 (9) (2000) 5435–5441.
[8] A. Saxena, A. Bishop, S. Shenoy, T. Lookman, Comput. Mater. Sci. 10 (1998) 16–21.
[9] S.H. Curnoe, A.E. Jacobs, Phys. Rev. B 64 (2001) 064101.
[10] F. Falk, Acta Metall. 28 (1980) 1773–1780.
[11] L.N. Trefethen, Spectral Methods in Matlab, SIAM, Philadelphia, 2000.
[12] Q. Alfio, S. Riccardo, S. Fausto, Numerical Mathematics, Springer-Verlag, Berlin, 2000.